Phase Diagram Modelling of Cast Energetic Materials

K.M. Jaansalu
Department of Chemistry and Chemical Engineering
Royal Military College of Canada
PO Box 17000 Stn Forces, Kingston ON, K7K 7B4, CANADA
kevin.jaansalu@rmc.ca

Abstract

The thermodynamic basis for the calculation of phase diagrams is reviewed with the intent to apply these principles to the three compounds TNT, RDX and HMX and the related binary phase diagrams. The thermochemical behavior of each compound is reviewed, focusing on the heat of fusion, transformation temperatures, and heat capacities of the relevant phases. The heat capacities of the supercooled liquid of both RDX and HMX were estimated. The calculated binary phase diagrams TNT – RDX and HMX – RDX compared favorably to literature data, highlighting the importance of heat capacity data in organic systems. A phase diagram for the TNT - HMX system was also calculated.

Introduction

Phase diagram modelling, as successfully applied to metallurgical systems, has not been applied to cast explosive formulations. New insensitive munitions contain formulations which consist of several compounds, as opposed to the relatively sensitive Composition B, which is based on the TNT / RDX binary system. A survey of the literature reveals that there is no open capability to generate or estimate phase diagrams of systems involving energetic materials. This lack of a phase diagram, or the capability to produce them, slows technological progress. As a result, a project was initiated to apply the principles of phase diagram modelling, which have been applied successfully to metallurgical systems for many years, to systems involving energetic materials.

What is important is the examination of all thermodynamic and phase diagram data to ensure a self-consistent set of equations that can be used to generate phase diagrams of multi-component systems. The interpretation of these diagrams result in the identification of critical points which then become subject to experiment. This process of modelling assists the experimentalist in identifying those regions that would be the most useful and beneficial. The initial effort is focused on modelling the HMX-RDX-TNT systems where the three constituent binary systems are reported in the literature.

Thermodynamic Basis: Pure Components

The thermodynamic relationships between the phases of the individual components can be derived from well-known and well-characterised parameters. For example, at the melting temperature, the solid is in equilibrium with the liquid. Thus, the Gibbs energy of the reaction from solid phase to liquid phase must be zero.

$$\Delta G = \Delta H_m - T_m \Delta S_m = 0$$

$$\Delta S_m = -\frac{\Delta H_m}{T_m} \qquad \text{Eq 1}$$

where ΔH_m is the heat required to melt the compound, T_m is the melting point, and ΔS_m is the entropy change on melting. Note that the enthalpy and entropy changes are positive values. Thus, the *difference* in Gibbs energy between the solid and liquid phases can be represented for all temperatures by:

$$\Delta G_{s \to l} = \Delta H_m - T \Delta S_m \qquad \text{Eq 2}$$

This effectively assigns the Gibbs energy of the solid a value of zero for all temperatures, but neglects any differences in the heat capacity between the two phases. This assignment is arbitrary and there is no difference to any other equation or form for the solid phase as long as the *difference* is preserved. However, it is by convention that the Gibbs energy of a pure component takes the form:

$$G = \Delta H_f^0 + \int_{T_{ref}}^{T} C_p dT - T\left(S_{ref}^0 + \int_{T_{ref}}^{T} \frac{C_p}{T} dT \right) \qquad \text{Eq 3}$$

wherein the enthalpy of formation, ΔH_f^0, absolute entropy, S_{ref}^0, (both at 298 K) and the heat capacity, C_p, are incorporated into the expression. Because the absolute entropy (not the entropy of formation) is used, the Gibbs energy expression above is sometimes termed the absolute Gibbs energy expression. Each phase of a component can have an energy expression, where at a certain transition temperature, the equations have equal values, and through appropriate manipulation, the heat of transition and the entropy of transition can be calculated. To give better extrapolations with temperature, expressions for the heat capacity of that particular phase can be included within these expressions.

The foundation of a phase diagram is then a sound understanding of the energy differences between phases of each pure component, even in the relatively simple case of solid and liquid where the differences are manifest in the heat of fusion, melting point, and the heat capacities of the solid and liquid.

Thermodynamic Basis: Solutions

Phase diagrams are concerned with solutions of components. These solutions may be solid, liquid, or even a gas. For a binary system at constant temperature, equilibrium between two phases, α and β, occurs when the partial molar Gibbs energy of each of the two components A and B are equal in both phases. That is:

$$\overline{G}_A^{\alpha} = \overline{G}_A^{\beta} \quad and \quad \overline{G}_B^{\alpha} = \overline{G}_B^{\beta} \qquad \text{Eq 4}$$

Generating the set of equations that allows the principle of chemical equilibrium to be used is well known in the literature (Pelton and Thompson, 1975, Kaufman and Bernstein, 1970). For any solution phase of A and B, the Gibbs energy per mole with respect to the selected reference states for each element can be represented by the equation:

$$\begin{aligned} G = {} & x_A G_A^{ref} + x_B G_B^{ref} + x_A G_A^{phase} + x_B G_B^{phase} \\ & + RT\left(x_A \ln x_A + x_B \ln x_B\right) \\ & + x_A x_B (p_0 + p_1 x_B + p_2 x_B^2 + ..p_n x_B^n ..) \end{aligned} \qquad \text{Eq 5}$$

where the first terms in the first line represent the energy associated with the reference state for elements A and B and the next two terms of the form $(G_B^{phase} = (h_B^t - Ts_B^t))$ represent the stabilities of A and B in this solution phase with respect to this reference state, often called the lattice stability. These four Gibbs energy expressions are derived after the form of equation 3 above. The second line is the ideal mixing term for a random substitutional solution, and finally the third line is a polynomial representation of the excess energy of mixing.

The corresponding partial molar properties are then represented by:

$$\overline{G_A} = RT\ln(x_A) + (h_A^t - Ts_A^t) + x_B^2\left((p_0 - p_1) + 2(p_1 - p_2)x_B + ..(n+1)(p_n - p_{(n+1)})x_B^n..\right) \quad \text{Eq 6}$$

$$\overline{G_B} = RT\ln(x_B) + (h_B^t - Ts_B^t) + x_A^2(p_0 + 2p_1x_B + 3p_2x_B^2 + ..(n+1)p_nx_B^n..) \quad \text{Eq 7}$$

These partial molar properties can be directly related to the activity of component B, relative to the reference state, through the relation:

$$\ln(a_B) = \ln(x_B) + \ln(\gamma_B) = \frac{\overline{G}_B}{RT} \quad \text{Eq 8}$$

By inspection of equations 7 and 8, the expression for the activity coefficient of B not only includes the excess energy, but the term ($G_B^{phase} = (h_B^t - Ts_B^t)$) that relates the phase of pure B to the reference state of pure B.

The third line in Equation 5 represents the excess energy of mixing which describes the extent of departure from the ideal behaviour as a function of composition. Commonly, these energy expressions are fit so that the calculated results are consistent with features of the phase diagram. There are various formalisms used and, although the form of these expressions may have a physical interpretation, the final form is always an analytical expression that gives the best fit for the data available.

The formalisms applied to organic systems (Oonk et al, 2004) are similar to those applied to metallurgical systems (Kaye et al, 2005). The formalism above is one derived by Margules, where the integral excess energy, G^E, is expressed as:

$$G^E = x_Ax_B(p_0 + p_1x_B + p_2x_B^2 + ..p_nx_B^n..) \quad \text{Eq 9}$$

If p_o is the only interaction parameter and is independent of temperature, the solution is said to be regular. If there are two parameters required, the solution is said to be sub-regular. The parameters, p_n, can vary with temperature:

$$p_n = h_n^E - Ts_n^E \quad \text{Eq 10}$$

For the n^{th} order G^E parameter, the first term represents an enthalpy of mixing parameter, the second term an excess entropy parameter. For metallurgical systems, the energy expressions can extend to three or four powers. In organic systems, the expressions have few terms as the magnitude of the interaction is much smaller.

The thermodynamic information required to reproduce known features of a binary phase diagram can be embodied within terms that have physical meaning, for example, enthalpy of mixing or fusion, or terms that result in low solubility in a (solid) solution phase. As such, the determination of the energy expressions can be guided by experimental measurements of key features, such as the eutectic temperature, where the equations for chemical equilibrium can be solved. However, before the solutions can be examined in any detail, the thermodynamic data for the pure components must be assessed and then the Gibbs energy expressions for the phases can then be derived. The mathematical operations are repetitive and onerous: perfectly suited to computer software. To this end, specialized software packages have been developed. In this work, the software suite FACT 2.2 (Bale et al, 1996) and FACTSage 6.4 (www.factsage.com) are used. The data is entered into a database after which various calculations are performed to produce the diagrams.

Thermodynamic Assessment: Pure Components

TNT

Starting with TNT, the literature was consulted for the melting point, the enthalpy of fusion, and heat capacities. The melting point and heat of fusion has been determined and reported by many researchers. For the purposes of this work, the melting point is taken to be 80.8°C (353.95K) and the heat of fusion is taken to be 23.1 cal g^{-1} (5250 cal mol^{-1}), in accordance with Urbanski (1988).

The literature was searched for the heat capacity; several reports and articles were located. Although the values of the heat capacities varied from worker to worker, as can be seen in Figure 1, the data have a common temperature dependence and similar change in the value of the heat capacity on melting. The data of Taylor and Rinkenbach (1924) and Cady and Rogers (1962) were determined using similar calorimetric methods, whereas all other data was determined using differential scanning calorimetry (DSC). In this regard, the data from Baytos (1979), being similar to that of Cady and Smith for the solid phase, will be used for the heat capacity of TNT for both the liquid and solid. Converting to a mole basis, with temperature in Kelvin, the expressions are:

$$C_P^{solid} = 11.174 + 0.17035T \text{ and } C_P^{liquid} = 140.61 + 0.12488T$$

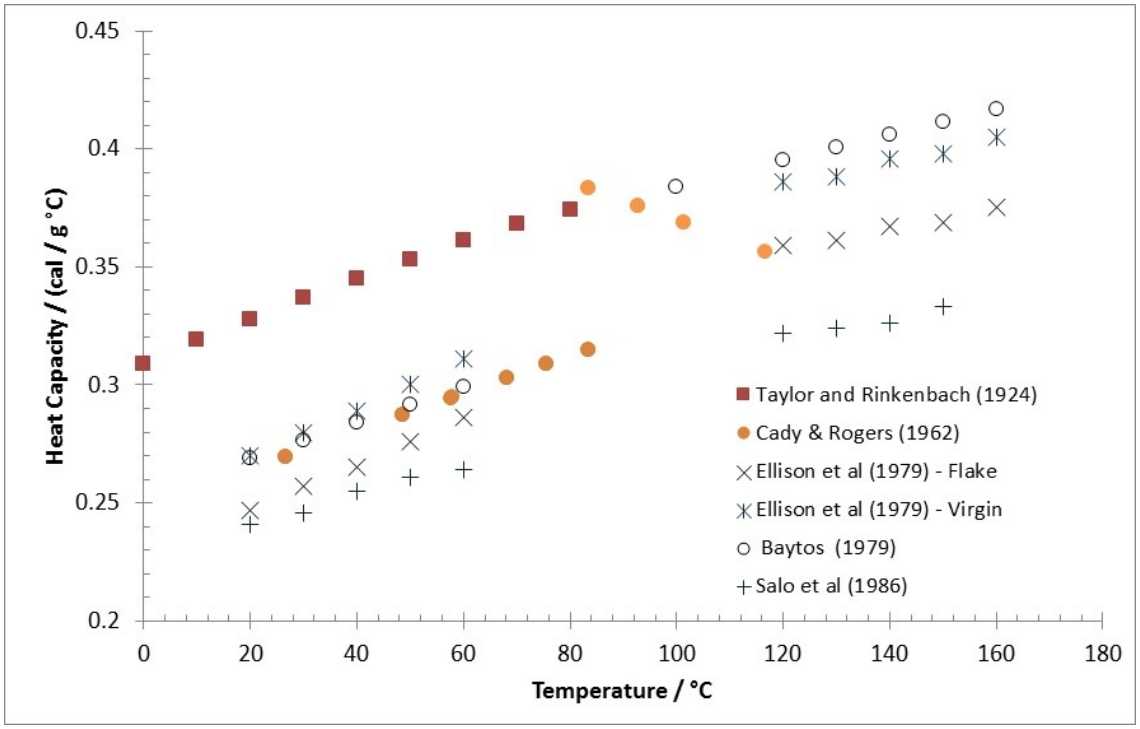

Figure 1: Heat capacity of TNT as a function of temperature.

As the amount of undercooling in these binary systems is expected to be small, no correction to the heat capacity expression for the undercooled liquid TNT will be made. An additional reason for using the data from Baytos is that the report also contains heat capacities for RDX and HMX, and it is likely that any systematic errors will be consistent across all these compounds.

RDX

The melting point of RDX is taken to be 205.3°C (478.45K) after Hall (1971) and McKenney and Krawietz (2003). The heat of fusion is taken to be 7356 cal mol^{-1} after McKenney and Krawietz as they determined this value from their experimental data and modeling work on the HMX-RDX phase diagram.

The heat capacity for solid RDX is taken from Baydos, which is reasonable when compared to other values in the literature (Krien et al, 1973, Cichinski et al, 1986). The data for the heat capacity for liquid RDX is inferred from the heat capacity data reported by Baydos for composition B above the melting point. The resulting temperature dependence is relatively high, but this behavior is expected for a heat capacity of a supercooled liquid. The lower limit for this heat capacity expression is where the heat capacity of the supercooled (metastable) liquid is the same as that of the solid RDX, which occurs at 92.92°C (~ $0.7T_m$ of RDX). The upper limit is taken to be the upper limit of the temperature range measured for composition B by Baydos, 157°C. This in turn gives a heat capacity of the liquid that remains higher than the solid by a factor of $2.22 \times \Delta S_{fus}$. At temperatures above 157°C (~ $0.9T_m$), the heat capacity has the same temperature dependence as the solid. The heat capacities are plotted as a function of temperature in Figure 2 below. The expressions are then:

$$C_P^{solid} = 7.489 + 0.15992\,T \;\; and$$
$$C_P^{liquid} = C_P^{solid}, \; for \; T < 366\,K$$
$$C_P^{liquid} = -187.294 + 0.693\,T, \; for \; 366\,K < T < 430\,K$$
$$C_P^{liquid} = 42.011 + 0.15992\,T, \; for \; 430\,K < T$$

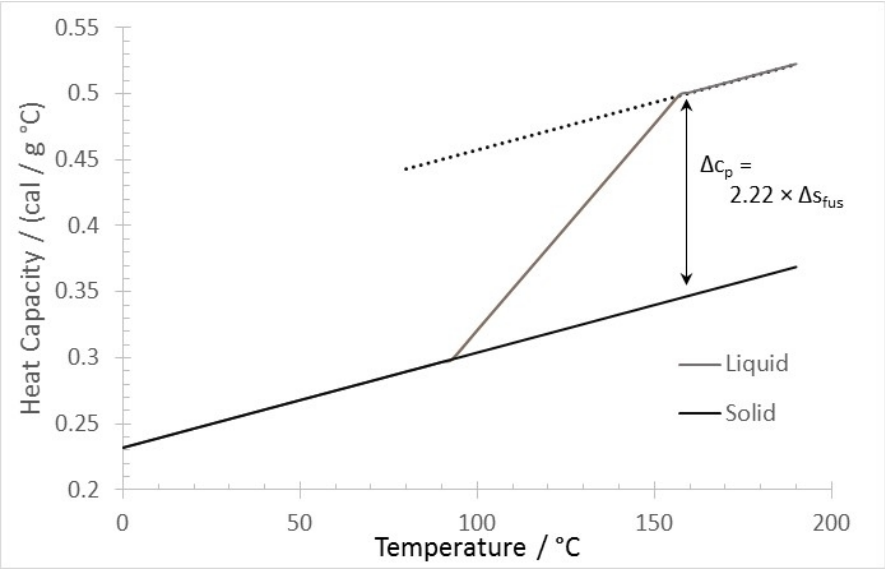

Figure 2: Heat capacity of RDX solid and liquid as a function of temperature.

HMX

The melting point of HMX is taken to be 280.5°C on the basis of the work by Cady and Smith (1962) and McKenney and Krawietz (2003). The heat of fusion of 9036 cal mol^{-1} is taken from McKenney and Krawietz. As noted above, their values are based on both experimental data and an assessment of the HMX-RDX phase diagram.

Of the three energetic compounds, only HMX has solid polymorphs, termed β, δ, α, and γ. The low temperature β form is desired due to the higher density and lower sensitivity (Cady and

Smith). The two phases which readily appeared in the work of McKenney and Krawietz were the β and δ forms. The γ form is metastable at all temperatures and pressures (McCrone 1965) and the α form has not been reported to appear in the melt casting of HMX containing explosives.

The transition temperature for the β → δ transformation has been determined by Cady and Smith (1962) to be 159°C and by Teetsov and McCrone (1967) to be 157°C, using different techniques. The value of 157°C is used in this work. The enthalpy of transformation has been determined by Hall (1971), Krien et al (1973), and McKenney and Krawitz (2003). Although the value determined by McKenney and Krawitz (2190 cal mol^{-1}) is slightly lower than that from the others (~2340 cal mol^{-1}), the lower value will be used to be consistent with other selected data above.

The heat capacity of HMX has been reported by several workers, and no agreement could be discerned. Krien et al (1973) and Carignan et al (1986) have found that the heat capacity for the δ form is higher than that of the β form. Conversely, the data published by Shoemaker et al (1985) and Rylance and Stubley (1973) indicate little difference in the heat capacity of these two forms. There is better a trend in that the temperature dependence of the heat capacity is very similar for all forms. This is to be expected as the different crystal forms are the result of different conformations of the molecule in the crystal structure (Wright, 1963). Without any strong evidence either way, the same heat capacity expression for all solids will be assumed, using the heat capacity of β form as determined by Baytos.

For liquid HMX, no heat capacity data could be located in the literature. As HMX and RDX are structurally and chemically similar, the heat capacity expression for the liquid is assumed to mimic that of RDX - that is, the heat capacity of the undercooled liquid is the same as the solid to $0.75T_m$, the heat capacity increases to a value of $2.22\Delta S_{fus}$ over that of the solid at $0.9T_m$, and then above $0.9T_m$, the heat capacity expression has the same temperature dependence as that of the solid. The resulting heat capacity expressions are:

$$C_P^{solid} = 23.916 + 0.1629\,T \;\; and$$
$$C_P^{liquid} = C_P^{solid}, \; for \;\; T < 415\,K$$
$$C_P^{liquid} = -157.419 + 0.600\,T, \; for \;\; 415\,K < T < 498\,K$$
$$C_P^{liquid} = 60.181 + 0.1629\,T, \; for \;\; 498\,K < T$$

Thermodynamic Results: Binary Phase Diagrams

TNT - RDX

This system forms the basis of the explosive formulation Composition B. The solid solubility of TNT in the RDX and RDX into TNT are expected to be small, and this is modelled by an equivalent Henrian activity coefficient that has the physical interpretation as the enthalpy of transformation of the solute phase into the same crystal form as the solvent, allowing for the ideal entropy of mixing. For solid TNT into solid RDX and vice versa, the value of 3100 cal mol^{-1} is used. These values affect the solid solubility but do not have a strong effect on the calculation of the eutectic temperature simply because the solubility is so low. The eutectic temperature is strongly affected by the excess energy term for the liquid phase, where a parameter of +1000 cal mol^{-1} was used.

The resulting phase diagram, along with experimental liquidus data, is presented below at Figure 3, followed by the TNT rich side at Figure 4 to better discern the experimental data around the eutectic. The calculated eutectic is at 79.3°C and at 3.47% RDX. The calculated RDX liquidus is in agreement with the data from Parker and Thorpe (1970) around the eutectic temperature. The discrepancy between the liquidus and the data from Campbell and Kushnarov (1947) can be reduced by altering the heat capacity of the liquid RDX. The assumed heat capacity for the liquid is too high as the change in heat capacity from a solid to a liquid is more likely to be equivalent to

a value between $0.5\Delta S_{fus}$ and ΔS_{fus} (Wu and Yalkowsky, 2009). For TNT, the change in heat capacity on melting is about $0.8\ \Delta S_{fus}$. Prior calculations for this system where the changes in heat capacity were not taken into account did not result in good agreement.

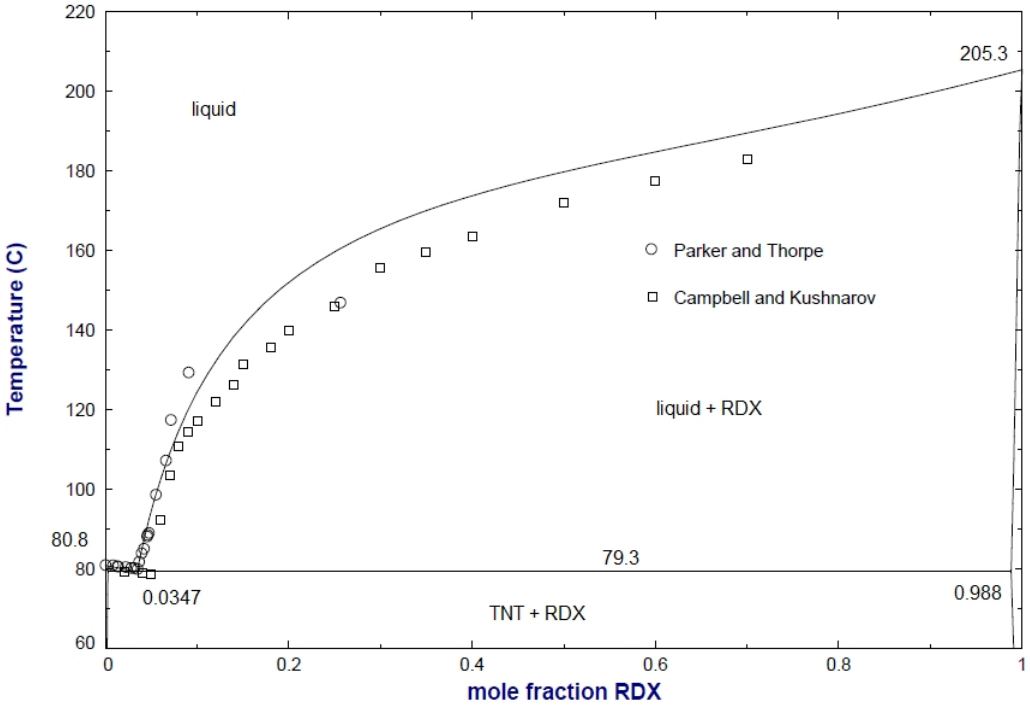

Figure 3: Calculated phase diagram of the TNT - RDX system.

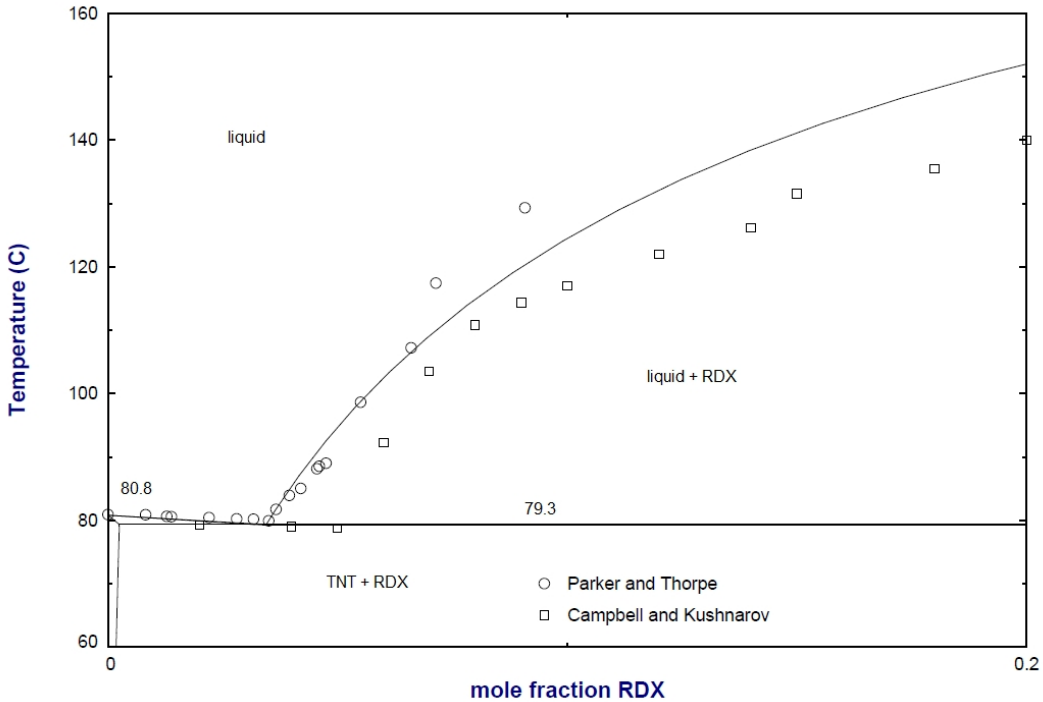

Figure 4: TNT side of the TNT - RDX phase diagram.

TNT-HMX

No experimental data could be located in the literature for this system, other than the accepted values of initial melting points of the eutectic of 79 to 80°C, and a maximum solubility of HMX of about 5% (Fedoroff, 1978). The Gibbs excess energy parameter for the liquid is +500 cal mol^{-1} in order to reproduce a eutectic temperature of 79.6°C and, similar to RDX above, a value of 3100 cal mol^{-1} is used for the lattice stability. The calculated phase diagram below at Figure 5 has the similar features to the diagram of TNT-RDX, which is to be expected. The eutectic composition is at 2.96% β-HMX.

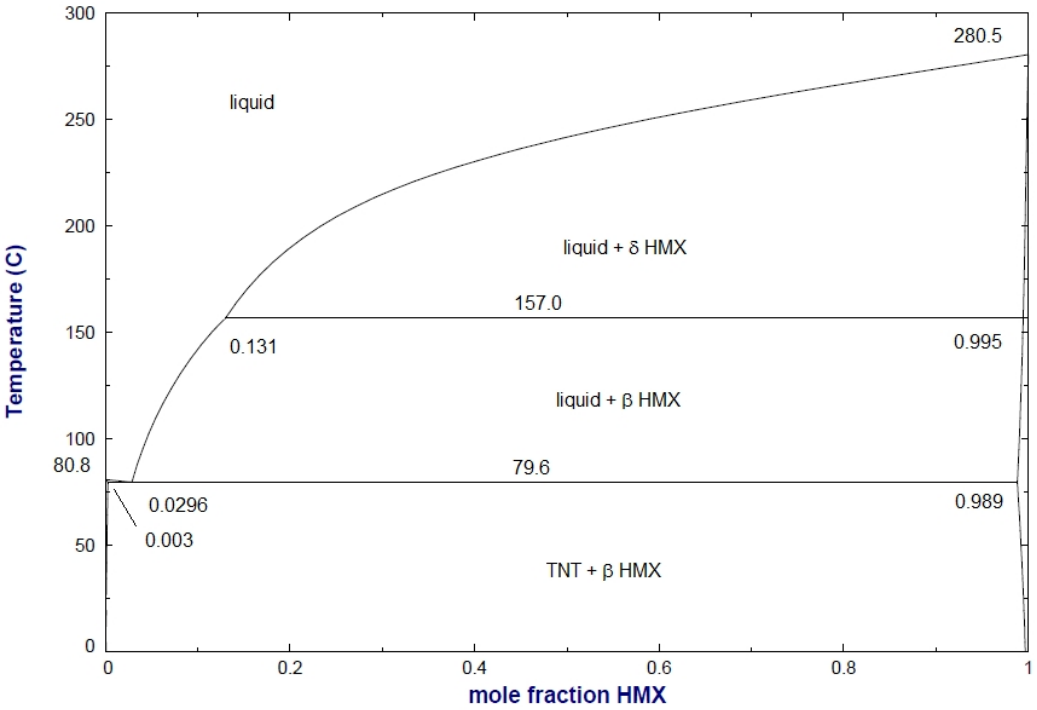

Figure 5: Calculated phase diagram of the TNT - HMX system.

HMX-RDX

This system has been well documented and modelled by McKenney and Krawietz in 2003. The experimental data and its interpretation is understandably complicated by the solid phase transformations of HMX. An excess energy parameter of +400 cal mol^{-1} is used in the calculation of the phase diagram. The lattice stabilities of RDX in both forms of HMX is 3100 cal mol^{-1}, and that for HMX in RDX is 4000 cal mol^{-1}. The phase diagram, at Figure 6, shows that δ-HMX forms a eutectic with RDX at 192.23°C and at a composition of 78.38% RDX. Included in the figure are the data points for the δ-HMX/ RDX eutectic and RDX liquidus reported by McKenney and Krawietz. These points are in modest agreement to their assessed temperature and composition of 191.4°C and 79.0 to 79.3% RDX.

Removing the δ-HMX from the calculation provides a phase diagram with β-HMX and RDX as the solid phases. Data points from McKenney and Krawietz are also plotted, where the open symbols represent the RDX liquidus and eutectic temperatures and the closed symbols represent the temperature for the onset of decomposition. The appearance of the liquid phase below the δ-HMX/ RDX eutectic is a metastable phenomenon -- the liquid should quickly transform to δ-HMX. However, this transformation must have been delayed by some nucleation barrier. McKenney and Krawietz did thermally cycle samples and showed that a eutectic between δ-HMX and RDX does appear when cycled above 193°C. The development of these thermodynamic models can be further used to provide the Gibbs energy differences of the phases (and compositions) at these

temperatures. This can give a better insight to the relative energetics involved in these transformations.

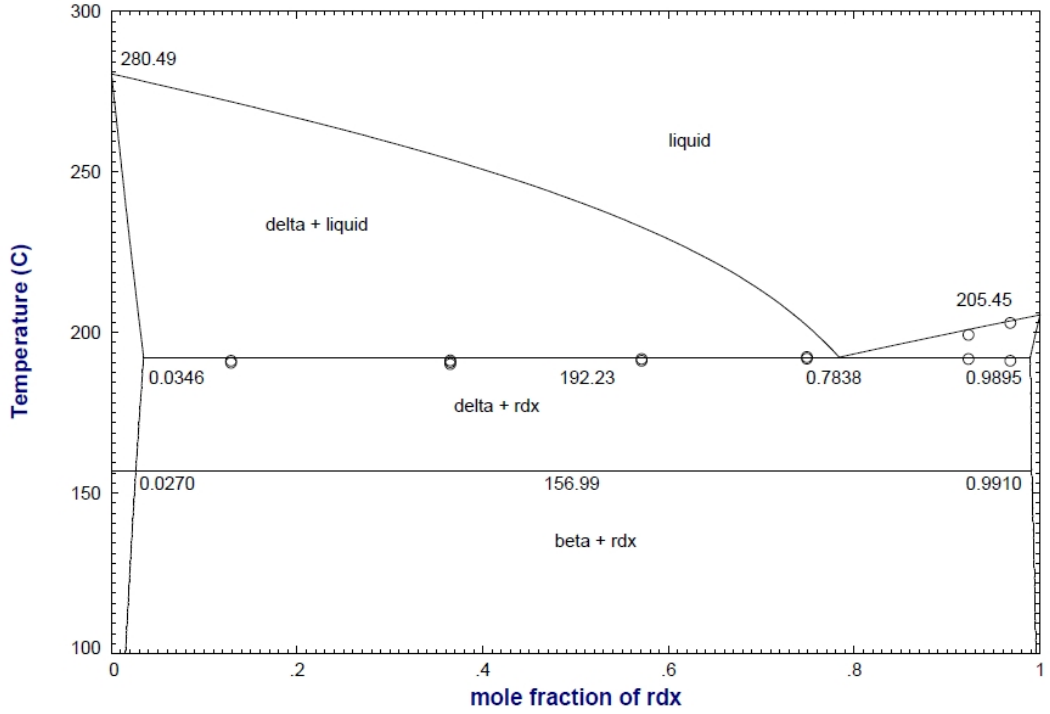

Figure 6: Calculated phase diagram of the HMX - RDX system, data points from McKenney and Krawietz.

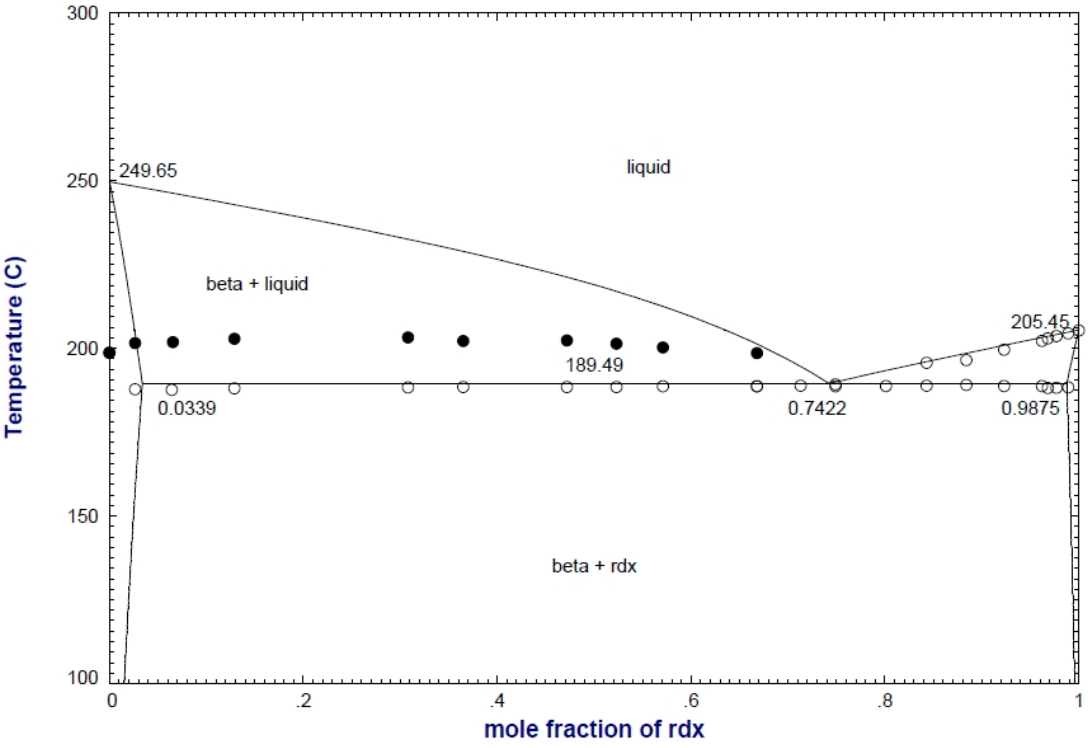

Figure 7: Calculated phase diagram of the metastable β -HMX - RDX system, data points from McKenney and Krawietz.

Discussion and Summary

This work is still very much in progress. One point that was encountered was that, unlike metallurgical systems, the change in heat capacity on melting (or any phase change) is important. This can be demonstrated by comparing the magnitude of the excess energy term for the liquid (here, a maximum of 0.25 * 1000 cal mol^{-1} or 250 cal for one mole) to the temperature range over which the difference in heat capacity applies (say 5 cal $mol^{-1}K^{-1}$ over 50 K, or 250 cal for one mole). Accounting for the change in heat capacity is a factor in the good agreement seen in the TNT – RDX system, but the agreement and estimation of the heat capacity expression can be improved for both HMX and RDX. However, locating or determining any data for the heat capacity for these undercooled liquids is problematic but worthy of pursuit.

Improvements in the data will result in better representation of the energy curves that underlie the phase diagram. An examination of their differences may provide insight as to the energetics behind the appearance of metastable melting, a phenomenon seen in the HMX – RDX system, and possible mechanisms for the energy or nucleation barriers to the transformation to the δ form of HMX.

This work was undertaken to determine those factors that are important in the computer calculation of phase diagrams of energetic materials. The important factors are the thermochemical properties of the materials, such as heats of transformation, heat capacities, and transformations temperatures. For RDX and HMX, the temperature dependence of the heat capacity for the supercooled liquid was estimated which resulted in reasonable reproductions of the TNT-RDX and HMX-RDX phase diagrams. The observed features in the phase diagram are more dependent on the thermal behavior of the pure components than on the factors that represent interactions in a solution. Further work will continue the theme of methods and models for heat capacities for undercooled liquids.

References

Bale, C.W., A.D. Pelton, W.T. Thompson, F*A*C*T 2.1 User Manual, Ecole Polytechnique de Montreal / Royal Military College of Canada, 1996.

Baytos, J.F, “Specific Heat and Thermal Conductivity of Explosives, Mixtures, and Plastic-Bonded Explosives Determined Experimentally,” LA-8034-MS, September 1979.

Cady, H.H., W.R. Rogers, “Enthalpy, Density, and Coefficient of Thermal Expansion of TNT,” LA-2696, July 1962.

Cady, H.H., L.C. Smith, “Studies on the Polymorphs of HMX,” LA-2652, May 1962.

Campbell, A.N., H.A. Kushnarov, “A Study of Systems Involving Trinitrotoluene, RDX, NENO, and Dinitrobenzene, with Particular Reference to the Composition of Binary Eutectics” Canadian Journal of Research, 25B, (1947) 216-227.

Carignan, Y, E.V. Turngren, C.T. Cichinski, J.K. Salo, “Thermodynamic Properties of Energetic Materials. IV Heat Capacity of Octahydro-1,3,5,7-tetranitro-1,3,5,7-tetrazocine Polymorphs,” Proceedings Thirteenth Symposium on Explosives and Pyrotechnics, Dec 2-4, 1986, pp. I25-I30.

Cichinski, C., J. Salo, E. Turngren, Y. Carignan, “Thermodynamic Properties of Energetic Materials. I. Heat Capacity of Hexahydro-1,3,5-Trinitro-1,3,5-Triazine (RDX),” Proceedings Thirteenth Symposium on Explosives and Pyrotechnics, Dec 2-4, 1986, pp. I13-I16.

Ellison, D.S., R.A. Alcorn, E. Neal, “Effects of Thermal Cycling on Trinitrotoluene and Tritonal Explosive Compositions” J Haz Mat, 4 (1980) pp. 57- 75.

Fedoroff, B.T., “Encyclopedia of Explosives and Related Items,” Vol VIII, U.S. Army Research and Development Command, Picatinny Arsenal, New Jersey, 1978, pp M57, O6.

Hall, P.G., “Thermal Decomposition and Phase Transitions in Solid Nitramines”, Transactions of the Faraday Society, 67 (1971) 556 – 562.

Kaufman, L. Bernstein, H. “Computer Calculation of Phase Diagrams: With Special Reference to Refractory Metals,” Academic Press, New York, 1970.

Kaye, M.H., K.M. Jaansalu, W.T. Thompson, “Condensed Phases of Inorganic Materials: Metallic Systems” in “Measurement of the Thermodynamic Properties of Multiple Phases: Experimental Thermodynamics Volume VII”, T. deLoos and R.D. Weir editors, Elsevier, Amsterdam, 2005.

Krien, G., H.H. Licht, J. Zierath, “Thermochemische untersuchungen an nitraminem”, Thermochimica Acta, 6 (1973) 465-472 (in German).

McCrone, W.C., “Polymorphism”, in Physics and Chemistry of the Organic Solid State, D Fox, M.M. Labes, and A. Weissberger, eds, John Wiley & Sons, New York, 1964, pp 725-767.

McKenney, R. L., T.R. Krawietz, “Binary Phase Diagram Series: HMX/RDX”, Journal of Energetic Materials, 21, 3 (2003) 141 – 166.

Oonk, H.A.J., J.Ll. Tamarit, “Condensed Phases of Organic Materials: Solid-Liquid and Solid – Solid Equilibrium” in “Measurement of the Thermodynamic Properties of Multiple Phases: Experimental Thermodynamics Volume VII”, T. deLoos and R.D. Weir editors, Elsevier, Amsterdam, 2005.

Parker, R.P., B.W. Thorpe, “The Phase Diagram of the RDX – TNT System,” Australia DSL Technical Report 140, January 1970.

Pelton, A.D., W.T. Thompson, “Phase Diagrams”, Progress in Solid State Chemistry, 10 (1975) 119-155.

Rylance, J., D. Stubley, “Heat Capacities and Phase transitions of Octahydro-1,3,5,7-tetranitro-1,3,5,7-tetrazocine (HMX)”, Thermichimica Acta, 13 (1975) 253-259.

Salo, J., C. Cichinski, Y. Carignan, E. Turngren, “Thermodynamic Properties of Energetic Materials. III Heat Capacity of Trinitrotoluene.” Proceedings Thirteenth Symposium on Explosives and Pyrotechnics, Dec 2-4, 1986, pp. I21-I24

Shoemaker, R.L., J.A Stark, L.G. Koshigoe, R.E. Taylor, “Thermophysical Properties of Propellants” Thermal Conductivity 18, Proceedings of the 18th International Thermal Conductivity Conference, Rapid City ND, (1985), pp 199-211.

Taylor, C.A., Wm. H. Rinkenbach, “The Specific Heats of Trinitrotoluene, Tetryl, Picric Acid and their Molecular Complexes,” Journal of the American Chemical Society, 46 (1924) 1504-1510.

Teetsov, A.S., W.C McCrone, “The Microscopical Study of Polymorph Stability Diagrams,” Microscope and Crystal Frontiers, 15 (1967) 13-29.

Urbanski, T.,“Chemistry and Technology of Explosives,” Volume 4, Pergamon Press, New York, 1988, as reprinted by Franklin Book Company, Elkins Park, PA, 1995.

Wright, G.F., “The Electrical Polarizabilities of Nitro Compounds”, in “Nitro Compounds,” T. Urbanski, ed., Proceedings of the International Symposium held at the Institute of Organic Synthesis, Polish Academy of Sciences. Warszawa, 18-20 September 1963, pp 159-176.

Wu, M., S. Yalkowsky, “Estimation of the Molar Heat Capacity Change on Melting of Organic Compounds”, Industrial and Engineering Chemistry Research, 48 (2009) 1063-1066.